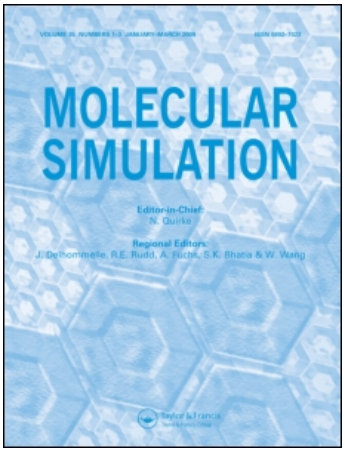

Molecular Simulation

Publication details, including instructions for authors and subscription information:
http://www.informaworld.com/smpp/title~content=t713644482

"Nanostructures in Thin-film Epitaxy: Exploring and Exploiting Substrate-mediated Interactions"

Michael L. Merrick[a]; Kristen A. Fichthorn[a]

[a] Department of Chemical Engineering, The Pennsylvania State University, University Park, PA, USA

To cite this Article Merrick, Michael L. and Fichthorn, Kristen A.(2004) '"Nanostructures in Thin-film Epitaxy: Exploring and Exploiting Substrate-mediated Interactions"', Molecular Simulation, 30: 5, 273 — 279

To link to this Article: DOI: 10.1080/08927020310001659151

URL: http://dx.doi.org/10.1080/08927020310001659151

Molecular Simulation, Vol. 30 (5), 30 April 2004, pp. 273–279

Taylor & Francis
Taylor & Francis Group

"Nanostructures in Thin-film Epitaxy: Exploring and Exploiting Substrate-mediated Interactions"

MICHAEL L. MERRICK* and KRISTEN A. FICHTHORN†

Department of Chemical Engineering, The Pennsylvania State University, University Park, PA 16802, USA

(Revised August 2003; In final form November 2003)

We review recent advances made in understanding the ramifications of substrate-mediated interactions for thin-film growth. Experimental studies and first-principles calculations with density-functional theory (DFT) indicate that substrate-mediated interactions can significantly influence thin-film growth. We review the findings from our kinetic Monte Carlo simulations used to model the growth of thin films, both with and without substrate-mediated interactions. For Ag heteroepitaxy on Pt(111), the pair interaction energies and adsorbate diffusion barriers were obtained from DFT calculations. Island densities for this system show significant deviations from what is predicted by classical nucleation theory. The electronic interactions created by the adsorbed atoms lead to the formation of repulsive barriers surrounding small islands and, as a result, sharp island-size distributions are produced. The island-size distributions can be manipulated by changing the growth conditions to yield desirable island sizes and shapes.

Keywords: Adsorbate interactions; Substrate-mediated interactions; Kinetic Monte Carlo; Thin-film growth

INTRODUCTION

Adsorbate–adsorbate interactions play a key role in controlling the morphology of thin films grown on solid surfaces. Traditionally, it is assumed that short-range attractive interactions are the main force governing the nucleation and the formation of islands. However, recent theoretical and experimental studies indicate that medium- and long-range interactions can be significant enough to influence the formation of nanostructures during thin-film epitaxy [1–9]. Despite the potential importance of medium- and long-range interactions, very little is known about the qualitative and quantitative impact these interactions have on the morphology in thin-film epitaxy. Kinetic Monte Carlo (KMC) simulations that utilize input from density-functional theory (DFT) calculations provide a tool that can probe the influence of adsorbate–adsorbate interactions on thin-film morphology. Using KMC, epitaxial growth is reproduced by the repeated advancement of the system to new states via the probabilistic choice of random events. The probability of choosing a certain event is proportional to its associated rate. The rate for a given event can be determined using transition-state theory (TST) with knowledge of the energy barrier and the attempt frequency. DFT calculations can provide the kinetic parameters needed to determine the rates for each event. Provided that enough rate processes are taken into account, a realistic description of growth can emerge. In this paper, we summarize our results from KMC simulation studies of the ramifications of substrate-mediated adsorbate interactions for the growth of Ag on a monolayer (ML) of Ag on Pt(111) [1,10,11].

BACKGROUND

Venables *et al.* [12] provide a full review of island nucleation and growth theories. Island formation can be divided into three distinct stages based on surface coverage: nucleation, growth and coalescence [12,13]. At low surface coverage, diffusion enables the aggregation of adsorbates into nuclei, which either dissociate if they are below the critical size, or later grow to become stable islands. As surface

*E-mail: mlm258@psu.edu
†Corresponding author. Tel.: +1-814-863-4807. Fax: +1-814-865-7846. E-mail: fichthorn@psu.edu

ISSN 0892-7022 print/ISSN 1029-0435 online © 2004 Taylor & Francis Ltd
DOI: 10.1080/08927020310001659151

coverage increases, it becomes more likely that deposited species will add to stable islands and promote island growth. In the final stages of submonolayer growth, the dominant process is the coalescence of two or more existing islands. A nucleation theory based on simple, mean-field rate equations is widely used to describe the stable density of two-dimensional islands in the island-growth regime [13,14]. In the island growth stage, mean-field nucleation theory takes the following form:

$$N_x \sim \left(\frac{F}{D}\right)^{\frac{i}{i+2}} \exp\left(\frac{-E_{d,i}}{k_B T}\right)^{\frac{1}{i+2}}, \quad (1)$$

where N_x is the stable island density, D is the hopping rate and, $E_{d,i}$ is the binding energy of an island of the critical size i [14]. From TST, the Arrhenius law gives the diffusion barrier:

$$D = \nu_0 e^{\frac{-E_b}{k_B T}}, \quad (2)$$

where E_b diffusion activation energy and ν_0 is the diffusion preexponential factor.

A major assumption in nucleation theory has been that interactions between adsorbed species do not exist beyond a short distance. However, experimental and theoretical studies detect the existence of strong interactions past the short range for some systems [1,5–8]. Decaying, oscillatory, charge-density waves associated with long-range electronic interactions have been experimentally imaged around adsorbed atoms and other surface defects in STM studies [5,6,15–18]. However, the long-range interaction is relatively weak compared to $k_B T$ for typical growth experiments. In the growth of Cu on Cu(111), for example, the long-range interaction energy is at most $\sim$2 meV at a distance of $\sim$2 nm from adsorbate [6]. By comparison, medium-range interactions quantified by DFT [1,7,8], can be strong enough to influence growth at experimental conditions. Recent experimental STM studies have detected a medium-range interaction [5,6] on Cu(111) and Ag(111). This interaction functions as an "extra" diffusion barrier for nucleation. The medium-range extra barrier for nucleation on Cu(111) occurs for adsorbate separations around 10 Å and has a magnitude of $\sim$15 meV [6]. This barrier is strong enough to influence growth at experimental conditions. In the growth of Ag on 1-ML-Ag/Pt(111), these interactions are believed to be responsible for the unusually high island densities observed experimentally in low-temperature STM studies [3]. However, to date, the effect of these interactions on island sizes and shapes has not been experimentally investigated.

METHODS

To investigate the ramifications of size- and shape-dependent "island barriers" for the formation of nanostructures on surfaces, we conduct KMC simulations of thin-film growth. We use the general method of Fichthorn and Weinberg [19] to simulate atom deposition with a rate of F (ML/s) onto an fcc(111) surface and adatom hopping from site i to site j with a rate $D_{i\to j}$ given by

$$D_{i\to j} = D_0\, e^{\left(\frac{-E_{i\to j}}{k_B T}\right)}. \quad (3)$$

The prefactor $D_0 = 10^{12}$/s is used to be consistent with DFT [20] results. The adatom-pair interactions were obtained from DFT calculations [1]. Figure 1 shows the pair interaction as a function of separation from a central adatom. This interaction is strongly attractive at the nearest-neighbor distance and repulsive at longer distances, forming a repulsive ring around the central adsorbate. The influence of adatom-pair interactions on adsorbate diffusion is included in the hopping barrier $E_{i\to j}$, which takes the form [1]

$$E_{i\to j} = E_b^0 + \frac{1}{2}(E_j - E_i), \quad (4)$$

where E_b^0(= 52 meV) [1] is the energy barrier for an isolated adatom to hop on an otherwise bare surface and $E_{i(j)}$ is the interaction energy (i.e. the sum of pair interactions) when an adatom is at site $i(j)$. As discussed elsewhere [11], we provide for island rearrangement by allowing atoms with one or more neighbors to execute hops beyond the nearest-neighbor distance. In this way, we mimic rapid, island-edge and corner diffusion, as well as concerted, many-atom processes that have been shown to contribute to island diffusion and rearrangement [2,21–23]. The inclusion of these

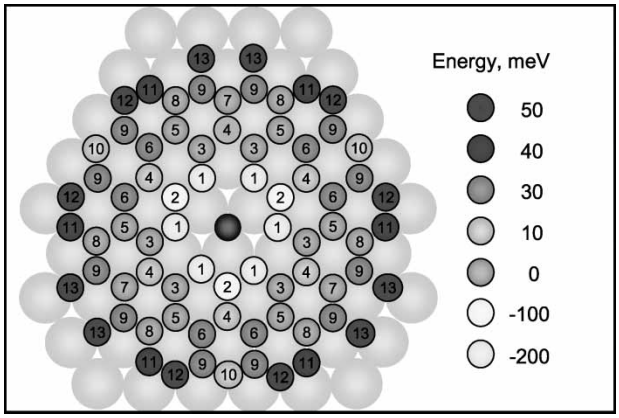

FIGURE 1 The electronic pair interaction energy (in meV) as a function of distance from a central adatom (shown as black circle) for Ag on strained Ag(111). Adapted from Ref. [1].

extra rate processes for island atoms allows for the formation of compact islands.

RESULTS

Comparisons between nucleation theory and simulated island densities reveal significant deviations. Using nucleation theory, the island density is calculated according to Eq. (1). In the low temperature regime, with the proportionality constant η, Eq. (1) takes the form

$$N_x = \eta\left(\frac{F}{D}\right)^{\frac{1}{3}}. \tag{5}$$

From KMC simulations, the island densities are found to be an order of magnitude or larger than predicted by nucleation theory (Eq. (5) with $\eta = 0.25$ [24]). The results, which span the temperature range of 40–85 K, are presented in Fig. 2. The island densities in Fig. 2 are determined in the beginning of the island growth regime, which typically occurs at a fractional surface coverage of 0.07. The simulations were performed on a 64×64 lattice with periodic boundary conditions. Finite-size effects are ruled out by comparing island-density results on a 64×64 lattice to those on a 128×128 lattice. The island densities from the two lattice sizes are within the statistical error of one another. The deviation from diffusion-limited nucleation theory, seen in Fig. 2, is the result of repulsive interactions surrounding the adsorbates (Fig. 1). The pairwise additive repulsive interactions inhibit adatoms from aggregating to form islands and a higher island density results.

Diffusion-limited nucleation theory predicts that island density should vary with a flux dependence of $F^{1/3}$. However, Fig. 2 shows only very weak flux dependence at the highest temperatures. At low temperatures, the island densities at different fluxes are indistinguishable from one another.

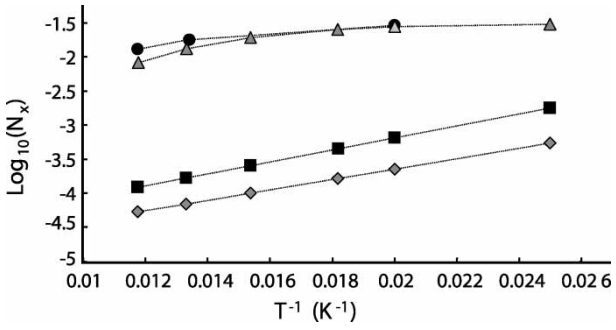

FIGURE 2 Arrhenius plot of the island density as a function of reciprocal temperature with $F = 0.1$ ML/s (circles) and $F = 0.01$ ML/s (triangles), and mean-field nucleation theory with $F = 0.1$ ML/s (squares) and $F = 0.01$ ML/s (diamonds). The lines are to guide the eye.

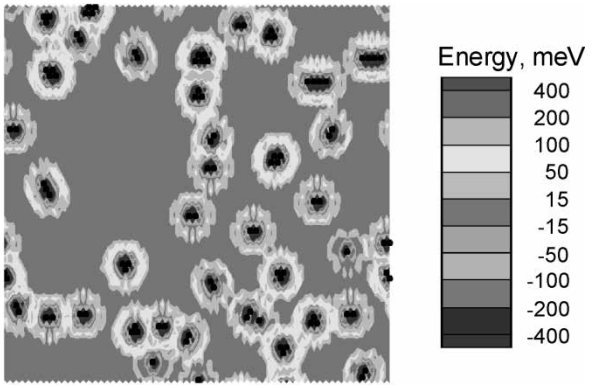

FIGURE 3 Simulation snapshot showing the pair interaction energy. The snapshot was obtained from a simulation at $T = 50$ K, $F = 0.01$ ML/s, and at a surface coverage of 0.024 ML. Full DFT interactions were used in the simulation.

Here, the energy needed to overcome the repulsive barrier is significantly larger than the thermal energy of the system. As a result, island nucleation via adatom diffusion does not occur. Adatoms must be deposited within the repulsive ring for island nucleation and growth to occur, leading to an independence of the results on flux.

The pairwise-additive interactions from neighboring adsorbates can combine constructively or destructively based on adsorbate separations. This can be seen in Fig. 3, which is a snapshot obtained from a KMC simulation at a coverage of 0.024 ML performed at $T = 50$ K and $F = 0.01$ ML/s. The image is created by placing a test particle at the empty sites and calculating the substrate-mediated interaction. The interaction energy is obtained by summing the individual pair interactions that each adsorbate casts on the surrounding sites. Figure 3 shows two important features of the interaction. First, as an island grows, the strength of the repulsive interaction surrounding the island also grows. Second, the interaction depends on the island shape.

The nucleation of two adsorbates results in the strengthening of the repulsive barrier, as seen in a comparison between Fig. 4(a) and (b). The magnitude of the repulsive interaction is further strengthened by the addition of more adsorbates to the island forming a chain-like structure [Fig. 4(c),(d)]. As seen in Fig. 4, the interactions strengthen the barrier around the island anisotropically creating a more repulsive area parallel to the chain's axis. If the island atoms are allowed to rearrange into a compact form, then the repulsion becomes nearly isotropic (Fig. 5).

Examination of the magnitude of the interaction surrounding some small islands yields critical island sizes, at which the repulsive barrier surrounding an island exhibits large changes. This can be seen in a comparison between the interactions surrounding a monomer, a dimer, and a compact trimer

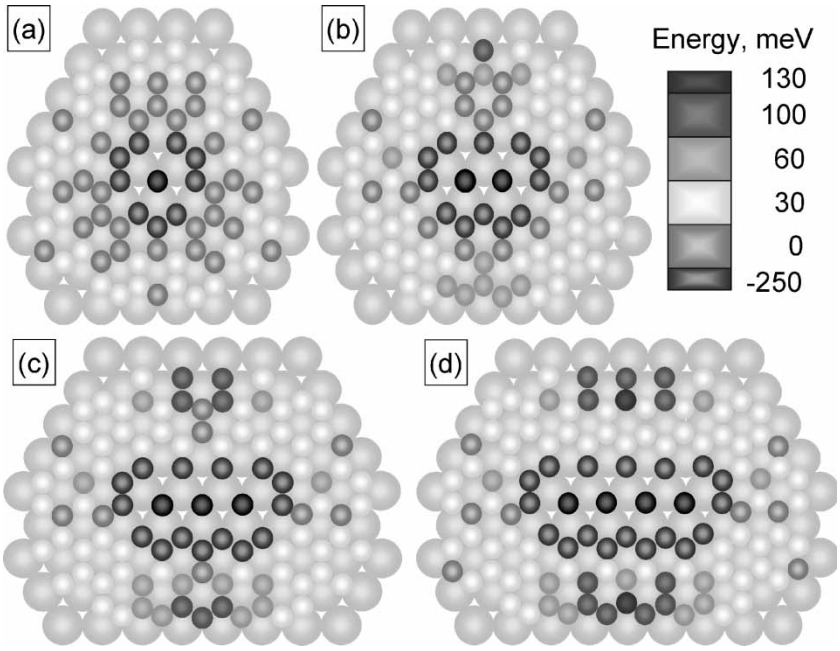

FIGURE 4 Potential-energy map for an adatom to approach another adatom (a), for an adatom to approach a dimer (b), a linear trimer (c), and a linear tetramer (d). The black circles represent adatoms and the large, purple circles represent surface atoms.

[Figs. 4(a),(b) and 5(a)]. In the case of the monomer and dimer, the repulsive interaction is in the 30–60 meV range. However, the addition of one more adsorbate to the dimer creates a compact trimer with a nearly isotropic repulsive interaction of 60–100 meV. Once the compact trimer has formed, the low-energy diffusion pathway that was available in the monomer and dimer (30–60 meV) no longer exists. The formation of a compact tetramer produces a surrounding topography similar to the trimer [Fig. 5(a),(b)]. Like the trimer, most of the sites surrounding the tetramer are in the 60–100 meV range. However, the fraction of sites with repulsion of 100–130 meV has increased. The pentamer [Fig. 5(c)], like the tetramer, still has the 60–100 meV pathway accessible, but now the fraction of sites lying in the 100–130 meV range increases. Once a hexamer has formed, the topography surrounding the island has become nearly isotropic with the interaction energy between 100 and 130 meV, with a few sites now in the 130 meV and greater range [Fig. 5(d)]. The compact heptamer [Fig. 5(e)] has a similar surrounding potential surface to that of the compact hexamer. However,

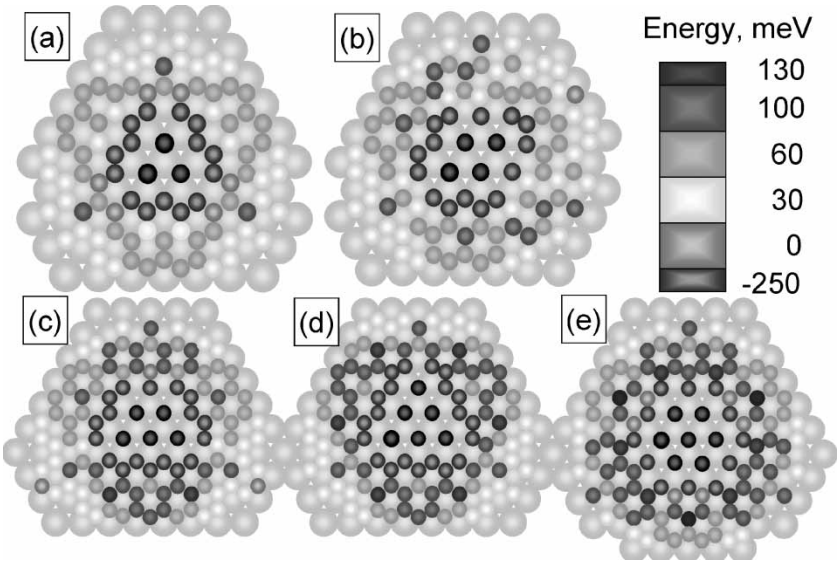

FIGURE 5 Potential-energy map for an adatom to approach a compact trimer (a), a compact tetramer (b), a compact pentamer (c), a compact hexamer (d), and a compact heptamer (e). The black circles represent adatoms and the large, purple circles represent surface atoms. (Colour version available online.)

the number of sites with repulsion above 130 has grown significantly. In a compact heptamer, repulsion of 170 meV is seen for the first time.

For the island sizes presented here, it is clear that the repulsive interaction continually increases in magnitude as the island grows in size. This results in a balance between the rate of diffusing over the repulsive barrier and the rate at which other adsorbates will nucleate with one another. At higher temperatures, the adsorbate will be increasingly likely to overcome the smaller barriers (as seen, for example, in the compact trimer, tetramer, and pentamer) and add to an existing island. As the island grows and produces a greater repulsive barrier, adsorbates will be less likely to add to the island and instead nucleate to form new islands.

Larger clusters complicate the analysis. For large clusters of a given size, a large variety of possible shapes exist. The analysis is further complicated by the significance of trio interactions. Since a considerable number of trio interactions can exist for large islands, even small trio interactions can significantly influence the potential-energy map. Nonetheless, for a reasonably compact island, when the number of atoms making up the island increases beyond ~ 12, one of the dimensions of the island will extend beyond the repulsive ring. Under these conditions, constructive interference of the repulsive interactions no longer occurs and the nearest-neighbor attractions could mitigate the intermediate-range repulsion.

In addition to significantly higher island densities, the presence of repulsive interactions gives way to unique island-size distributions. In Fig. 6, the island-size distribution is presented for two models, a system with DFT interactions and a system with only a nearest-neighbor attractive interaction. The results are obtained from simulations performed at $T = 35\,\mathrm{K}$, $F = 0.01\,\mathrm{ML/s}$, and at a surface coverage of 0.07 ML, which marks the beginning of the island growth regime. The system with only the nearest-neighbor attraction was simulated on a 512×512 lattice and the results represent the average of 28 runs. In increasing the number of runs from 20 to 28, the uncertainty decreased by a value of 0.001. The system with DFT interactions was simulated on a 64×64 lattice and the results represent the average of 20 runs. The error for this set of results is $\sim 0.1\%$.

As seen in Fig. 6, the size distribution is significantly sharper for the system with medium-range interactions; the system with only nearest-neighbor attraction has a size distribution approximately one order of magnitude broader. Island sizes range from 2 to 10 for the system with medium-range interactions and 2–90 without these interactions. The sharpness of the size distribution for the system with interactions is the result of a balance between the thermal energy of the adsorbate and the magnitude of the repulsive barrier. As adsorbates add to islands, the repulsive interactions combine constructively to increase the magnitude of the repulsive barrier. At a fixed temperature the adsorbates will continue to add to an island until the repulsive barrier surrounding the island becomes larger than the thermal energy of the adsorbate. At this point, diffusion over the repulsive barrier becomes slower than deposition and the island fails to grow, thus creating islands of a similar size.

The potential-energy surface significantly changes when comparing islands of sizes 2 and 3–5 and 6 (Figs. 4 and 5). These radical jumps in the potential energy surface can also be detected in island-size distribution plots. Figure 7 shows the island-size distribution at two test conditions. The black bars in Fig. 7 show an island-size distribution obtained from the average of 128 simulation runs on a 64×64 lattice at $T = 40\,\mathrm{K}$, $F = 0.01\,\mathrm{ML/s}$, and a coverage of 0.07 ML. Islands of size 3, 4, and 5 represent 72% of the islands on the surface. The gray bars in Fig. 7 show an island-size distribution obtained from the average of 74 simulation runs on a 64×64 lattice at $T = 50\,\mathrm{K}$, $F = 0.01\,\mathrm{ML/s}$, and a coverage of

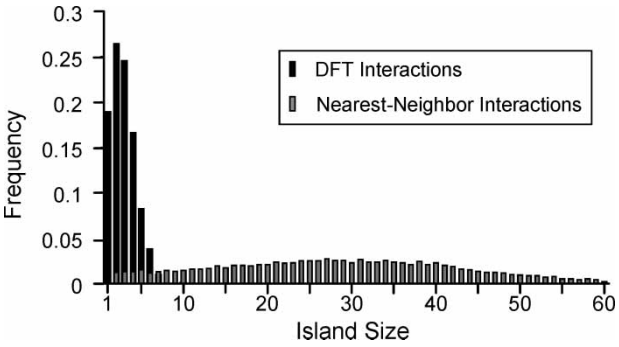

FIGURE 6 Island-size distributions at $F = 0.01\,\mathrm{ML/s}$, $T = 35\,\mathrm{K}$, and a surface coverage of 0.07 ML from the DFT-KMC model (black bars) and from a KMC simulation with only rearest-neighbor attraction (gray bars).

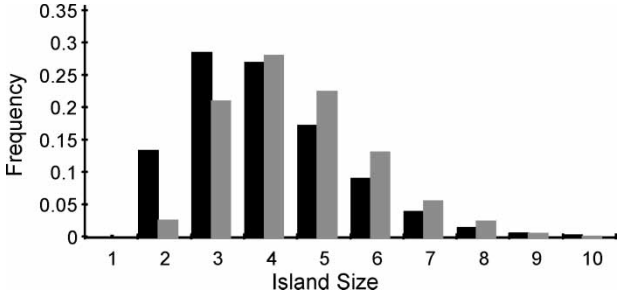

FIGURE 7 Island-size distribution at $F = 0.01\,\mathrm{ML/s}$ for $T = 40\,\mathrm{K}$ (black bars) and for $T = 50\,\mathrm{K}$ (gray bars) at a surface coverage of 0.07 ML. At $T = 40\,\mathrm{K}$, islands of size 3, 4, and 5 make up 72% of the total islands on the surface. At $T = 50\,\mathrm{K}$, islands of size 3, 4 and 5 make up 75% of the total islands on the surface.

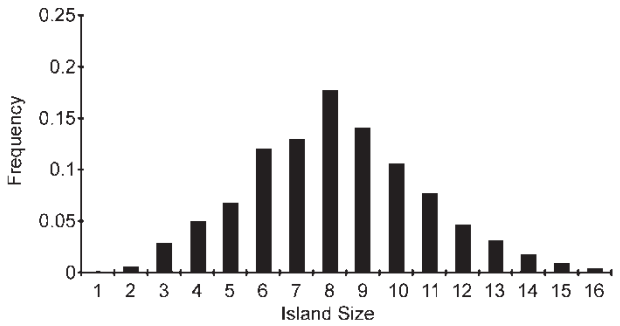

FIGURE 8 Island-size distribution at $F = 0.01\,\mathrm{ML/s}$, $T = 65\,\mathrm{K}$, and at a surface coverage of 0.07 ML. Islands of size six atoms and larger compose 85% of the total islands on the surface.

0.07 ML. At these conditions, islands of size 3, 4, and 5 compose 75% of the islands on the surface. In this figure, the 3–4–5 grouping is clearly separated from islands of size 2 and 6.

Figure 8 shows an island-size distribution obtained from an average of 68 simulation runs on a 64×64 lattice at $T = 65\,\mathrm{K}$, $F = 0.01\,\mathrm{ML/s}$, and a coverage of 0.07 ML. Islands containing six atoms make up 12% of the total number of islands on the surface. However, only 6% of the islands on the surface are size 5. For these growth conditions, the higher temperature and lower deposition rate favor islands containing between 6 and 11 atoms.

The dependence of the average island size $<S>$ on the temperature and deposition rate is summarized in Fig. 9. The insensitivity of $<S>$ to deposition rate at low temperatures confirms the inability of adatoms to diffuse over the repulsive barrier and add to the island. However, as the temperature is increased, island growth is mediated to an increasing extent by adatom diffusion over the island's repulsive barrier. This causes the stronger temperature dependence of $<S>$ at higher temperatures.

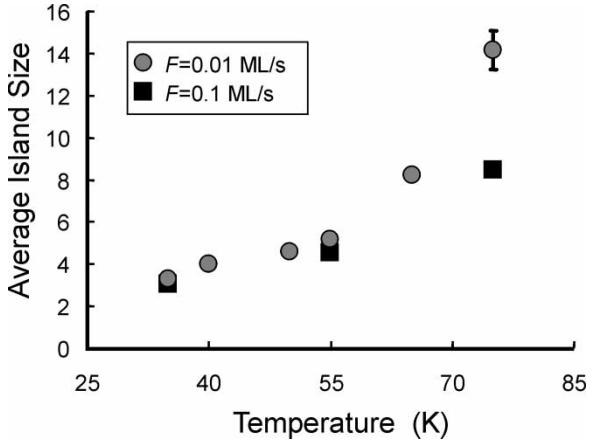

FIGURE 9 Average island size as a function of temperature. Error bars included unless smaller than data point.

At higher temperatures, the deposition rate has a greater effect on $<S>$. At the lower flux, more diffusion steps can occur on the time scale of deposition and as a result more adatoms can overcome the repulsive barrier surrounding islands.

CONCLUSION

In this paper, we presented a review of our work [1,10,11] using first-principles DFT calculations and kMC simulations to study thin-film growth. When adsorbate interactions exist beyond the short range, their effect on the growth morphology can be significant. For the heteroepitaxial growth of Ag on Pt(111), we presented our finding showing the deviations from diffusion-limited nucleation theory for this system. We find higher island densities and significantly sharper island-size distributions than predicted by the theory. Such studies, with increasingly accurate atomic-scale detail, have significant potential for enhancing our understanding of thin-film growth.

Acknowledgements

The authors are supported by NSF grants ECC-0085604 and DGE-9987589.

References

[1] Fichthorn, K.A. and Scheffler, M. (2000) "Island nucleation in thin-film epitaxy: a first-principles investigation", *Phys. Rev. Lett.* **84**, 5371.
[2] Ovesson, S., Bogicevic, A., Wahnstrom, G. and Lundqvist, B.I. (2001) "Neglected adsorbate interactions behind diffusion prefactor anomalies on metals", *Phys. Rev. B* **64**, 125423.
[3] Brune, H., Bromann, K., Roder, H., Kern, K., Jacobsen, J., Stoltze, P., Jacobsen, K. and Norskov, J. (1995) "Effect of strain on surface diffusion and nucleation", *Phys. Rev. B* **52**, R14380.
[4] Michely, T., Langerkamp, W., Hansen, H. and Busse, C. (2001) "Comment on dynamics of surface migration in the weak corrugation regime", *Phys. Rev. Lett.* **86**, 2695.
[5] Repp, J., Moresco, F., Meyer, G. and Rieder, K.H. (2000) "Substrate mediated long-range oscillatory interaction between adatoms: Cu/Cu(111)", *Phys. Rev. Lett.* **85**, 2981.
[6] Knorr, N., Brune, H., Epple, M., Hirstein, A., Schneider, M.A. and Kern, K. (2002) "Long-range adsorbate interactions mediated by a two-dimensional electron gas", *Phys. Rev. B* **65**, 11542.
[7] Bogicevic, A., Ovesson, S., Hyldgaard, P., Lundqvist, B.I., Brune, H. and Jennison, D.R. (2000) "Nature, strength, and consequence of indirect adsorbate interactions on metals", *Phys. Rev. Lett.* **85**, 1910.
[8] Ovesson, S. (2002) "Mean-field nucleation theory with non-local interactions", *Phys. Rev. Lett.* **88**, 116102.
[9] Venables, J.A. and Brune, H. (2002) "Capture numbers in the presence of repulsive adsorbate interactions", *Phys. Rev. B* **66**, 195404.
[10] Fichthorn, K.A., Merrick, M.L. and Scheffler, M. (2003) "Nanostructures at surfaces from substrate-mediated interactions", *Phys. Rev. B* **68**, 041404(R).

[11] Fichthorn, K.A., Merrick, M.L. and Scheffler, M. (2002) "A kinetic Monte Carlo investigation of island nucleation and growth in thin-film epitaxy in the presence of substrate-mediated interactions", *Appl. Phys. A* **75**, 17.
[12] Venables, J.A., Spiller, G.D.T. and Hanbucken, M. (1984) "Nucleation and growth of thin films", *Rep. Prog. Phys.* **47**, 399.
[13] Brune, H. (1998) "Microscopic view of epitaxial metal growth: nucleation and aggregation", *Surf. Sci. Rep.* **31**, 121.
[14] Venables, J.A. (1973) "Rate equation approaches to thin film nucleation kinetics", *Philos. Mag.* **27**, 697.
[15] Crommie, M.F., Lutz, C.P. and Eigler, D.M. (1993) "Imaging standing waves in a two-dimensional gas", *Nature* **363**, 524.
[16] Avouris, Ph. and Lyo, I.W. (1994) "Observation of quantum-size effects at room temperature on metal surfaces with STM", *Science* **264**, 942.
[17] Jeandupeux, O., Burgi, L., Hirstein, A., Brune, H. and Kern, K. (1999) "Thermal damping of quantum interference patterns of surface-state electrons", *Phys. Rev. B* **59**, 15926.
[18] Avouris, Ph., Lyo, I.W. and Molinasmata, P. (1995) "STM studies of the interaction of surface state electrons on metals with steps and adsorbates", *Chem. Phys. Lett.* **240**, 423.
[19] Fichthorn, K.A. and Weinberg, W.H. (1991) "Theoretical foundations of dynamic Monte-Carlo simulations", *J. Chem. Phys.* **95**, 1090.
[20] Ratsch, C. and Scheffler, M. (1998) "Density-functional theory calculations of hopping rates of surface diffusion", *Phys. Rev. B* **58**, 13163.
[21] Ruggerone, P., Ratsch, C. and Scheffler, M. (1997) "Growth and properties of ultrathin epitaxial layers", In: King, D.A. and Woodruff, D.P., eds, *The Chemical Physics of Solid Surfaces* (Elsevier, Amsterdam) **Vol. 8**, p 490.
[22] Yu, B.-D. and Scheffler, M. (1997) "*Ab initio* Study of step formation and self-diffusion on Ag(100)", *Phys. Rev. B* **55**, 13916.
[23] Miron, R.A. and Fichthorn, K.A. (2001) "The step and slide method for finding saddle points on multidimensional potential surfaces", *J. Chem. Phys.* **115**, 8742.
[24] Bales, G.S. and Chrzan, D.C. (1994) "Dynamics of irreversible island growth during submonolayer epitaxy", *Phys. Rev. B* **50**, 6057.